Parts Orienting with Shape Uncertainty

Srinivas Akella
Beckman Institute
University of Illinois, Urbana-Champaign
Urbana, IL 61801

Matthew T. Mason
School of Computer Science
Carnegie Mellon University
Pittsburgh, PA 15213

Abstract

Parts manufactured to tolerances have shape variations. Most work in robotic manipulation assumes that part shape does not vary. Orienting devices such as bowl feeders frequently fail due to variations in part shape. In this paper we develop techniques to orient parts with shape uncertainty. We present a shape uncertainty model and describe the nondeterminism in parts orienting that arises from shape uncertainty. We characterize a class of parts that can be reliably oriented with sensor-based and sensorless orienting plans under shape uncertainty. We present implemented planners that generate orienting plans for the entire variational class of part shapes given a nominal part shape and shape uncertainty bounds. We describe experiments to demonstrate generated plans and outline issues for future work.

1 Introduction

Parts manufactured to tolerances have variations in shape. However most work in robotic manipulation assumes the part shape is known exactly and that parts have no shape variations. Orienting devices such as bowl feeders often fail due to variations in part shape. Developing techniques to manipulate parts in the presence of shape uncertainty is important. We study the effects of uncertainty in part shape on orienting and identify conditions under which we can generate orienting plans for parts with shape uncertainty. The variations in the shape of a part are characterized by the part's nominal shape and shape uncertainty bounds. The *variational class* (Requicha [18]) of parts for a nominal part shape under a given model of shape uncertainty is the class of all part shapes that satisfy the shape uncertainty bounds. Given a nominal part shape and shape uncertainty bounds, we wish to generate orienting plans for the variational class of parts.

Part shape critically influences the orientability of parts (e.g., Goldberg [11]; Caine [6]; Akella and Mason [3]). The challenge of part shape uncertainty is to find plans that orient the infinite set of part shapes that are valid instances of a given variational class. The main results of this paper are:

1. The operational effect of shape uncertainty on parts orienting is to introduce nondeterminism.
2. Both sensor-based and sensorless plans to orient parts with shape uncertainty exist.
3. We have implemented planners and demonstrated parts orienting in the presence of shape uncertainty.

After outlining related work, we review our previous work on orienting parts with known shape using partial sensor information. We present a shape uncertainty model and discuss the nondeterminism in parts orienting due to shape uncertainty. After sketching a method to determine the set of stable edges for the input shape uncertainty, we focus on the class of parts with a constant set of stable edges. We describe sensor-based and sensorless planning and characterize planner properties. We outline a planner for parts whose set of stable edges may change due to shape uncertainty. We present experimental results and conclude with a discussion of future work.

This paper summarizes work presented in (Akella [1]).

2 Related Work

The need to manufacture parts specified by tolerances arose with mass production methods that required interchangeable parts. Voelcker [20] surveys the area of tolerancing and describes the trend towards mathematically based tolerancing standards. Requicha [18] developed a mathematical formalism of tolerance zones to describe the valid variational class of parts and offset operations to generate these tolerance zones. Current tolerancing and dimensioning standards include the ASME Y14.5M-1994 standard [4]. Yap [21] advocates the use of computational geometry techniques and exact computation for tolerancing metrology.

Donald [9] was the first to explicitly consider shape uncertainty for a manipulation problem. He defined a "generalized configuration space" with additional dimensions for the parametric variations in part features and used it to generate multiple-step compliant motion strategies. Brost [5] developed a polygon-based tolerance zone model and has used it to design 3-D part fixtures that are robust to variations in part shape. Latombe *et al.* [14] present an assembly sequencing algorithm to determine if an assembly sequence exists for all instances of the components within the specified tolerances, and to generate it when it exists. They assume part edges vary only in position and not in orientation. Joskowicz *et al.* [12] compute the variations in kinematic behavior of mechanisms from the tolerance specifications of their

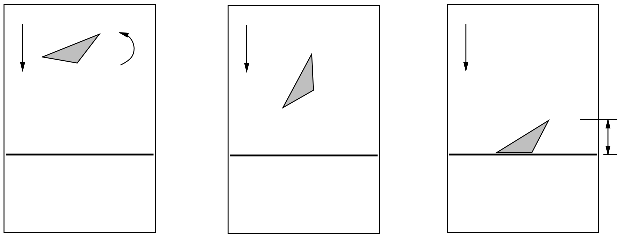

Figure 1: Schematic overhead view of a part on a conveyor during a push-align operation. The conveyor motion is "downward".

parts. Kavraki [13] presents a vector field for orienting parts and establishes its stability for toleranced parts.

Recently Chen *et al.* [7] developed algorithms for sensorless feeding and fixturing of shape toleranced parts. For feeding with fences, their tolerance model assumes vertices, defined relative to the center of mass, lie inside vertex uncertainty disks. They use Chen and Ierardi's ([8]) algorithm to generate sensorless plans for a class of polygons. They also compute the maximum uncertainty disk radius for which a plan exists.

Our work relies on previous results on the mechanics and planning of pushing and grasping operations (Mason [15], Goldberg [11]). It is also related to AND/OR search based planning for sensor-based manipulation (Taylor *et al.* [19]) and sensor-based orienting of multiple parts by parallel-jaw grasping (Rao and Goldberg [17]).

3 Orienting Parts with Known Shape

We summarize our previous work on orienting parts with known shape (Akella [1]; Akella and Mason [3]) to provide the necessary background. We use sensors that provide partial information on part orientation along with mechanical operations to generate orienting plans. We focus on an implementation where a part in an unknown initial orientation drifts on a conveyor belt until it contacts a frictionless fence placed perpendicular to the conveyor motion (Figure 1). The part rotates until one of its edges is aligned with the fence. An LED sensor measures the diameter of the aligned part perpendicular to the fence. An orienting plan is a conditional sequence of *push-align operations* executed to orient the part. Each push-align operation is an action followed by a sensor reading. The action consists of the robot picking up an aligned part at the fence by suction, rotating the part by a chosen angle, and releasing it on the conveyor to be aligned at the fence. The sensor measures the part diameter after alignment to distinguish the orientations. Orienting a part means identifying the part edge aligned against the fence.

When a part on the moving conveyor contacts the fence, it is pushed normal to the fence face. The radius function (Goldberg [11]) predicts the part rotation due to such a linear normal push. The *radius function* of a polygon is a mapping from the orientation ϕ of a supporting line of the polygon to the perpendicular distance r from the polygon center of mass to the supporting line. The local minima of the radius function correspond to stable edges of the part. An edge is *stable* if the center of mass projects onto the edge interior, and is *unstable* if the center of mass projects outside the edge. A part rotates to achieve a minimum radius, and comes to rest with only stable edges aligned with the fence. A push maps the entire interval between two local maxima to the enclosed stable orientation.

The *resting range* of a stable edge is the set of initial part orientations for which the part comes to rest on the edge. The limits of a resting range are specified by the part orientations at which the fence is perpendicular to the line connecting the center of mass and the appropriate transition vertices. A *transition vertex* is a vertex that corresponds to a local maximum in the radius function. An *action range* is an interval of rotation angles for which a part transitions from one edge to another, and is obtained from the resting ranges.

We have shown that sensor-based and sensorless plans exist to orient parts up to symmetry in their push-diameter and push functions, and implemented planners to generate such plans. We proved that sensor-based plans require $O(m)$ operations, where m is the maximum number of states with the same sensor value.

4 Orienting Parts with Shape Uncertainty

We describe our shape uncertainty model and the effects of shape uncertainty on parts orienting.

4.1 Shape Uncertainty Model

We use a shape uncertainty model that explicitly bounds the locations of the vertices and center of mass since they are critical in determining part behavior during a push. It is defined by the following assumptions (Figure 2).

- The nominal part shape, defined by the positions of the vertices and center of mass, is known.
- All parts are convex polygons that remain convex for all instantiations of the shape uncertainty values.
- Each vertex lies inside a circle of radius r_v centered at its nominal location.
- The center of mass lies inside a circle of radius r_c centered at its nominal location. The center of mass location and the radius r_c can be specified, or computed as functions of r_v and the polygon shape if we assume uniform mass density.
- The vertex uncertainty circles do not intersect each other and do not intersect the center of mass uncertainty circle. Each uncertainty circle intersects only the two edges incident at that vertex.
- The actual part edges are straight lines connecting the actual vertex positions.

Any part shape that belongs to the set of shapes defined by the nominal shape and the shape uncertainty model is a

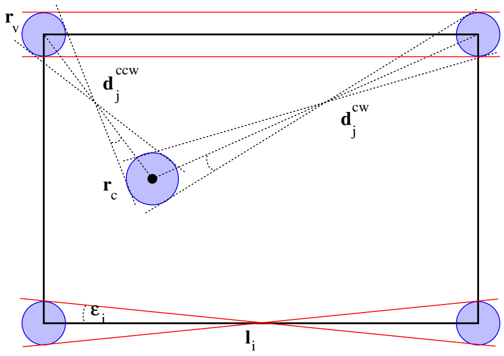

Figure 2: Shape uncertainty model showing uncertainty bounds on locations of the center of mass and vertices. The nominal center of mass and polygon edges are drawn bold. The extremal positions and orientations of the longest edges are also shown.

member of the variational class of parts to be oriented. This shape uncertainty model permits the following variations, which can be computed in terms of the shape uncertainty parameters (Figure 2):

1. *Variations in orientations of part edges.* The extremal orientations of a stable edge are determined from the tangents to the vertex uncertainty circles. The edge orientation varies between $\psi - \epsilon$ and $\psi + \epsilon$ where ψ is its nominal orientation, $\epsilon = \sin^{-1}(2r_v/l)$, and l is the nominal edge length.
2. *Variations in the diameter values of the stable orientations.* The diameter of the aligned part normal to the fence can vary from its nominal size d so it lies in the interval $[d - 2r_v, d + 2r_v]$.
3. *Variations in the action ranges.* The action ranges are obtained from the resting ranges. The uncertainty in the resting range limits (Figure 3) can be determined from the angles defined by the common tangents to the center of mass uncertainty circle and the vertex uncertainty circles for the clockwise (CW) and counterclockwise (CCW) vertices of the edge.
4. *Variations in the center of mass location.* Computing the exact center of mass uncertainty locus for a part with shape uncertainty assuming uniform mass density is an open problem. See (Akella [1]) for a discussion on bounding the center of mass locus with a circle.
5. *Variations in the set of stable edges.* The set of stable edges of a part may vary with the center of mass location and the edge positions and orientations.

4.2 Nondeterminism

The main operational effect of shape uncertainty on parts orienting is to introduce nondeterminism arising from variations in part geometry. The actions for a particular instantiation of a part shape are deterministic. Over the variational class of parts however, some actions appear nondeterministic. An action applied to different part instantiations in the

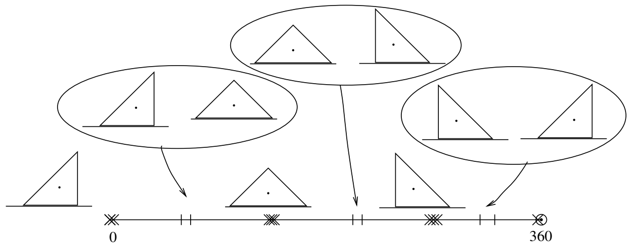

Figure 3: Resting ranges for an isosceles right triangle with shape uncertainty. The stable states for each initial part orientation are shown. The uncertainty in the stable orientations and the resting ranges is indicated by the x's and vertical bars respectively drawn at their extremal orientations. r_v and r_c are 0.4 mm and the length of the hypotenuse is 22.63 mm.

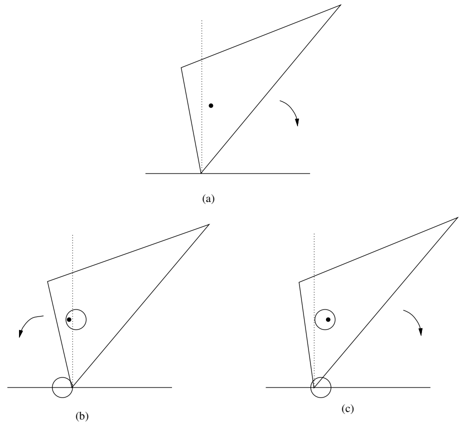

Figure 4: Shape uncertainty results in nondeterministic actions. The result of the push depends on the center of mass and contact vertex locations. The dotted line is the contact normal. (a) For the nominal part shape, the part rotates CW since the center of mass is to the right of the normal. (b) This part instantiation rotates CCW. (c) This part instantiation rotates CW.

same initial orientation can result in different outcomes (Figure 4). The action is deterministic for each instantiation, but must be treated as a nondeterministic action since it has different outcomes over the variational class of part shapes.

The set of stable edges may also vary over the variational class of parts. Edges of a part that are stable in its nominal shape may become unstable for some instantiations of the part, or unstable edges of the part may become stable (Figure 5). These variations in the set of stable edges also manifest themselves as nondeterministic behaviors. We next tackle the problem of identifying edge stability.

4.3 Edge Stability Regions

The set of stable edges depends on the location of the center of mass relative to the edges. The *stability region* of a part edge is the region of center of mass locations for which the edge is stable. It is the region in the polygon interior for which the center of mass projects onto the interior of the edge segment. See Figure 6. Uncertainty in the length, position, and orientation of an edge and in the position of the center of mass leads us to replace the stability region with two

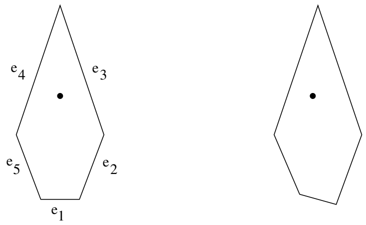

Figure 5: Edges of a part can become stable or unstable depending on the instantiation of the shape uncertainty values. Edge e_1 is stable for the nominal part shape at left and unstable for the instantiation at right. Edges e_2 and e_5 are always unstable, and edges e_3 and e_4 are always stable for the specified shape uncertainty values.

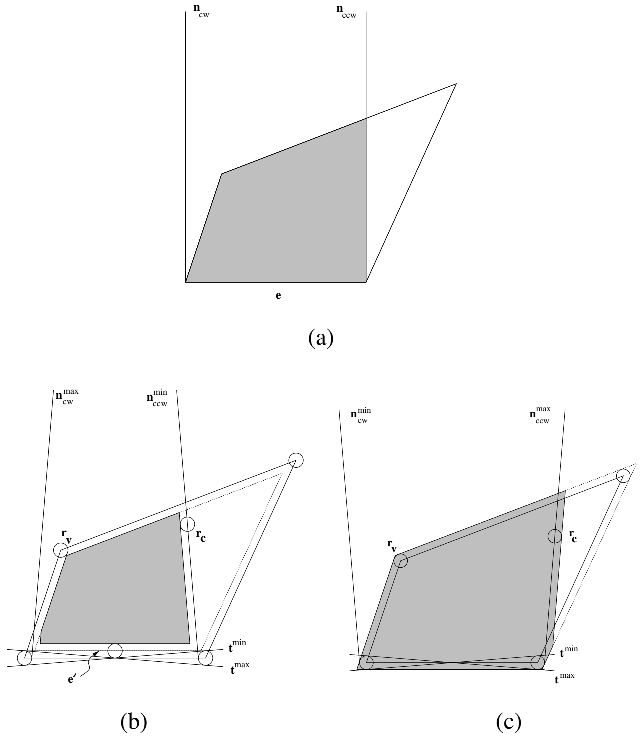

Figure 6: Stability regions of the bottom edge e of the polygon. (a) Stability region with no shape uncertainty. (b) Shrunken stability region. (c) Expanded stability region. The shrunken and expanded stability regions shown approximate the true regions.

similar constructions. The *shrunken stability region* of an edge is the region of center of mass locations in the polygon interior for which the edge is always stable. The *expanded stability region* of an edge is the region of all center of mass locations in the polygon interior for which the edge may be stable. If the center of mass is outside the expanded stability region of an edge, the edge is always unstable. When the center of mass is outside the shrunken stability region and inside the expanded stability region, we refer to the edge as a *sometimes-stable* edge since its stability depends on the part instantiation.

For a part with n edges, we can compute conservative approximations of these regions for an edge in $O(n)$ time using region intersection and union operations as described in (Akella [1]). Point-inclusion tests (Preparata and Shamos [16]) can determine in $O(n)$ time the stability regions the nominal center of mass belongs to and classify an edge as always stable, always unstable, or sometimes-stable.

We refer to a part with a constant set of stable edges as a part with a *single qualitative shape*. Such a part has its center of mass inside the shrunken stability regions of all edges, or inside shrunken stability regions of stable edges and outside the expanded stability regions of the remaining edges for the specified shape uncertainty values. For a part with a single qualitative shape, we next describe how to generate sensor-based orienting plans.

5 Sensor-Based Orienting

A sensor-based orienting plan measures the part diameter after every push. The sensor consists of two parallel arrays of LEDs and phototransistors perpendicular to the fence on either side of the conveyor. To deal with variations in the diameter values due to shape uncertainty, we find the valid set of diameter values for each state and then find the corresponding set of sensor values consistent with the sensor. Two states are considered *indistinguishable* if their sets of sensor values intersect. An *indistinguishable set* is a set of states where each state is indistinguishable from at least one other state. A sensor-based plan for a part with shape uncertainty must distinguish any initial indistinguishable set for all part shapes that belong to the variational class.

5.1 Representative Actions

We first compute a finite set of *representative actions* for a set of states. Consider determining the range of actions to transition from state s_i to state s_j without shape uncertainty. Let the stable orientation of s_i be ψ_i, and the right and left limits of the resting range of s_j be ρ_j and λ_j. Any action in the interval $(\lambda_j - \psi_i, \rho_j - \psi_i)$ causes a deterministic transition from s_i to s_j. Shape uncertainty introduces nondeterminism in the actions. To compute the deterministic and nondeterministic action ranges for an edge, we find the smallest and largest rotations guaranteed to achieve the transition to each destination edge, and the smallest and largest rotations that can potentially achieve the transition to each destination edge. We assume the start edge can be in any valid orientation, each vertex can be at any position in its uncertainty circle, and the center of mass can be at any position in its uncertainty circle.

Now consider transitioning from s_i to s_j with shape uncertainty. The variations in the stable orientation and in the resting range of an edge can be determined from the uncertainty circles of the center of mass and its transition vertices. The stable orientation ψ_i varies between $\psi_i^{min} = \psi_i - \epsilon_i$ and $\psi_i^{max} = \psi_i + \epsilon_i$ (Figures 2 and 7). The right limit of the resting range of state s_j varies between $\rho_j^{min} = \rho_j - sin^{-1}((r_v + r_c)/d_j^{cw})$ and $\rho_j^{max} =$

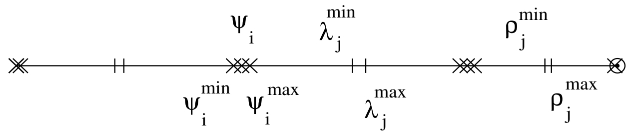

Figure 7: Illustration of the uncertainty in stable orientations of state s_i and uncertainty in resting ranges of state s_j.

$\rho_j + sin^{-1}((r_v + r_c)/d_j^{cw})$, where d_j^{cw} is the distance from the center of mass to the CW transition vertex of edge e_j. The minimum and maximum left limits λ_j^{min} and λ_j^{max} are computed similarly. The action range specified by the open interval $(\lambda_j^{max} - \psi_i^{min}, \rho_j^{min} - \psi_i^{max})$ guarantees a deterministic transition from s_i to s_j (Figure 8). A deterministic action range is an equivalence class of actions.

Nondeterministic action ranges are action ranges with multiple possible outcomes. A nondeterministic action causes a transition from a start edge to a destination edge or to the stable edges adjacent to the destination edge. We compute the nondeterministic action ranges from state s_i that can lead to state s_j or its CW or CCW stable neighbors, s_j^{cw} and s_j^{ccw} respectively. The part transitions from s_i to either s_j or s_j^{ccw} over the action range specified by the closed interval $[\lambda_j^{min} - \psi_i^{max}, \lambda_j^{max} - \psi_i^{min}]$, and from s_i to either s_j or s_j^{cw} over the action range $[\rho_j^{min} - \psi_i^{max}, \rho_j^{max} - \psi_i^{min}]$. See Figure 8. A nondeterministic action range is not guaranteed to be an equivalence class of actions.

The deterministic and nondeterministic action ranges for a state cover the action space (Figure 9). To find the action ranges of a set of states, we overlap the deterministic and nondeterministic action range intervals of each state in the set to obtain another set of intervals, the *overlap ranges*. Deterministic overlap ranges are formed by the overlap of only deterministic action ranges and nondeterministic overlap ranges are formed by the overlap of one or more nondeterministic action ranges. Representative actions for the set of states are selected from each of these overlap ranges.

5.2 Planning and Plan Existence

We generate plans that minimize worst-case length by breadth-first AND/OR search (Akella [1]). We compute and apply representative actions for each indistinguishable set encountered during the search process. If a plan exists, it is guaranteed to work for any instance of the part since it works under the most extreme combination of center of mass, vertex, and edge placements. See Figure 10 for an example plan. Bounds on the plan length obtained for parts with known shape (Akella and Mason [3]) do not apply to parts with shape uncertainty.

We show with an example that some parts may not have a guaranteed orienting plan for some small value of the shape uncertainty parameters. Consider a rectangle whose length is slightly greater than its breadth, and whose center of mass is slightly off-center. This nominal shape can be brought to a distinct orientation. A valid instantiation of the part with

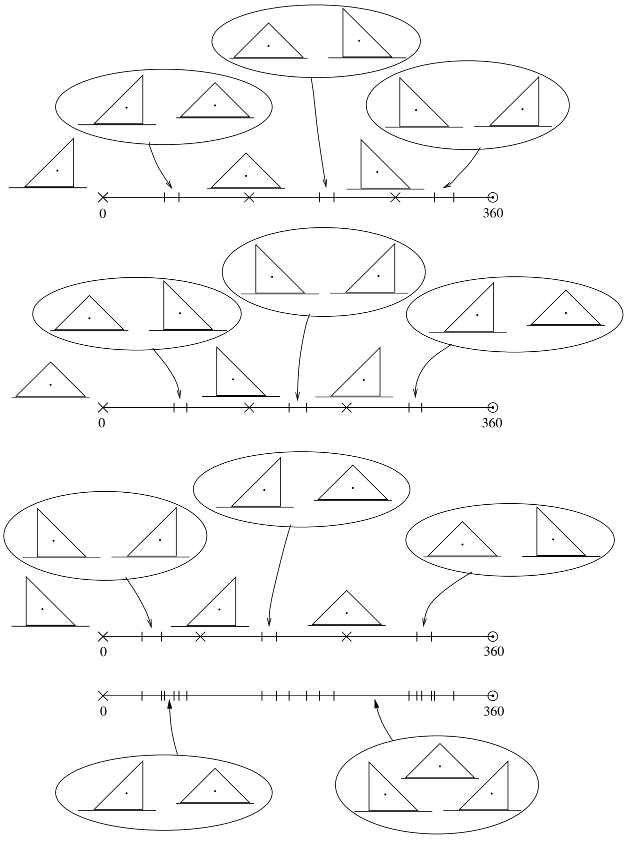

Figure 8: Action ranges for the stable edges of an isosceles right triangle with shape uncertainty, computed from the resting ranges in Figure 3. The action range limits are marked by vertical bars and the nominal stable orientations are marked by x's. An action from a deterministic action range causes a transition to a single state while an action from a nondeterministic range can cause a transition to either of two states. The overlap ranges are shown at bottom.

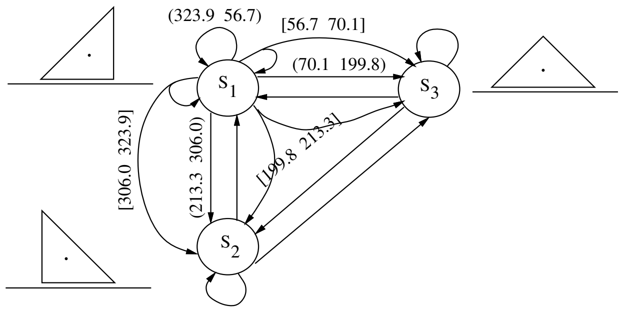

Figure 9: Transition graph of the isosceles right triangle with nondeterministic and deterministic arcs. Nondeterministic arcs are shown only for transitions from state s_1. r_c and r_v are 0.4 mm.

shape uncertainty is a square with its center of mass at its center, which can be oriented only up to symmetry.

Any part with at least one stable edge with a unique diameter value can always be oriented. To see this, note that it is sufficient to bring the part to the stable edge with the unique diameter to orient it. A randomized plan (Erdmann [10]) can repeatedly choose random rotations of the part until it comes

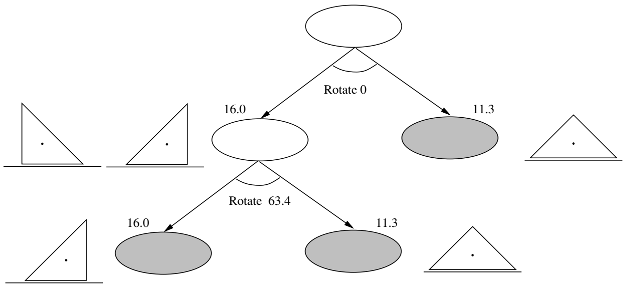

Figure 10: Sensor-based plan to orient the isosceles right triangle when r_v and r_c are 0.4 mm. Nodes contain indistinguishable states and each set of arrows linked by an arc represents a push-align operation. Shaded goal nodes have a single state. The sensor value at a node indicates the diameter value for the indistinguishable set.

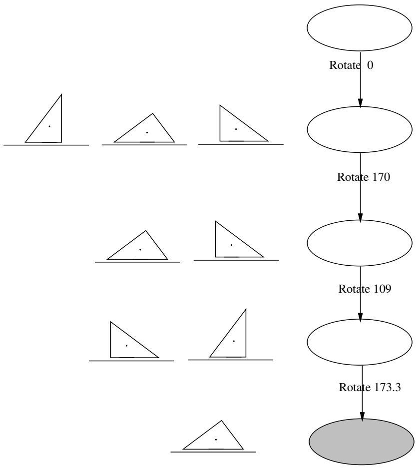

Figure 11: Sensorless plan to orient a triangle. r_c and r_v are 2 mm, the longest triangle edge has length 63.2 mm.

to rest on the stable edge with the unique diameter. However there is no finite bound on the length of the plan.

6 Sensorless Orienting

Interestingly, we can perform sensorless orienting with shape uncertainty. Sensorless plans, which must bring all possible initial orientations to the same goal orientation, are generated using breadth-first search in the space of representative actions. See Figure 11 for an example plan. For a single qualitative shape, the set of stable edges is constant and only the size of the resting ranges changes. This suggests that a polynomial-time algorithm (Goldberg [11]) can generate sensorless orienting plans with shape uncertainty.

7 Are the Planners Complete?

We first address completeness of the sensor-based planner. Given a nominal part shape with bounded shape uncertainty, does the planner always return an orienting plan when one exists and indicate failure when no plan exists? Since the planner performs breadth-first search in the space of representative actions, the planner is complete if the computed action ranges are accurate. If the action ranges are overly conservative, the planner may not find a solution even when one exists.

When generating the action ranges for a stable edge, we assumed that each stable edge can take any allowed orientation and that the center of mass and the transition vertices can be located anywhere in their uncertainty circles. However each part instantiation is a shape with constraints on the orientations and positions of the part edges. Specifying the orientation of a stable edge whose action ranges we wish to find constrains the positions of only its vertices. Any other vertex can assume any position in its uncertainty circle. So the action ranges from a stable edge to all stable edges other than its adjacent edges are accurately determined. For transitions from the stable edge to its adjacent edges, we can find the extremal position ranges of the vertices for each orientation of the edge and compute the corresponding action range. If we compute the union of the action ranges over all orientations of the edge, we obtain the maximal action range for the transition to an adjacent edge. The action ranges to adjacent edges computed under our assumption of independence of edge orientations and vertex positions are more conservative than those from this procedure.

The computed center of mass locus also influences the accuracy of the action ranges. We have assumed the center of mass locus is a circle, when in fact it may not be a circle (Akella [1]). The circumscribing circle we use may be an overly conservative approximation of the true locus.

These two sources of inaccuracy in the action ranges suggest the sensor-based planner may not be complete. A generated plan is guaranteed to orient any instance of the part. When the planner cannot find a plan however, it is unclear if there exist part instantiations that cannot be oriented. Completeness of the sensorless planner, as with the sensor-based planner, depends on the accuracy of the action ranges.

8 Qualitative Shape Changes

We have so far assumed the set of stable edges is constant over all instantiations of the shape uncertainty parameters. When the set of stable edges changes due to shape uncertainty, a part behaves qualitatively differently. For example, a part with two stable edges in its nominal shape may have three stable edges for some instantiations. We refer to a part whose set of stable edges can vary as a part with *multiple qualitative shapes*. A plan generated for one qualitative shape of the part may fail for another qualitative shape (Figure 12). Multiple qualitative shapes occur in these cases:

1. Center of mass is inside shrunken stability regions of stable edges, inside expanded stability regions of some edges while outside their shrunken stability regions, and outside expanded stability regions of remaining edges. See example in Figure 5.

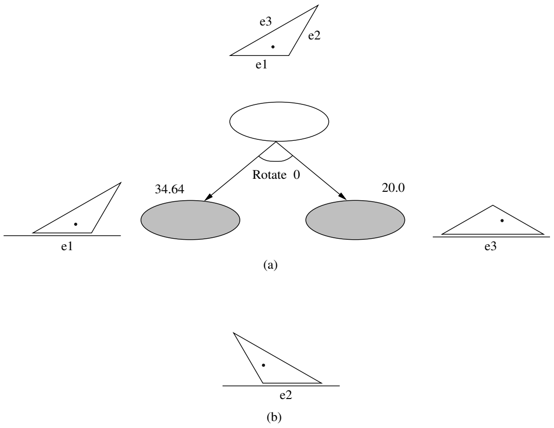

Figure 12: The effect of qualitative shape changes due to shape uncertainty. (a) Orienting plan for the nominal part shape. Edges e_1 and e_3 are stable and edge e_2 is unstable. The longest edge e_3 has length 69.28 mm. (b) For shape uncertainty values r_v and r_c of 2 mm, e_1 and e_3 are always stable and e_2 is stable for some instantiations of the shape and has the same diameter value as e_1. The plan fails when it cannot distinguish edges e_1 and e_2.

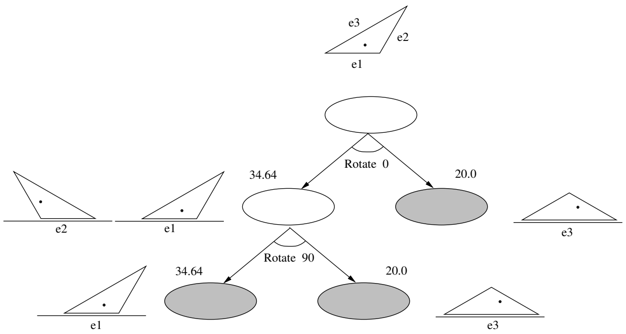

Figure 13: A plan that works for the triangle of Figure 12 even with qualitative shape changes.

2. Center of mass is outside shrunken stability regions of all edges, inside expanded stability regions of some edges, and outside expanded stability regions of remaining edges.

Each qualitative shape is defined by all the stable edges and a subset of the sometimes-stable edges. We identify the set of stable, unstable, and sometimes-stable edges by performing the point-inclusion test for the center of mass with the shrunken and expanded stability regions of every edge.

8.1 Generating Plans

Plans that work even in the presence of qualitative shape changes can sometimes be found (Figure 13). Qualitative shape changes modify the orienting problem to one with multiple transition graphs, where each transition graph represents a different qualitative shape of the part. We have to determine the action ranges associated with the arcs of the graphs and perform planning in the space of these multiple graphs. A guaranteed orienting plan is one that can orient every part shape corresponding to any of the graphs.

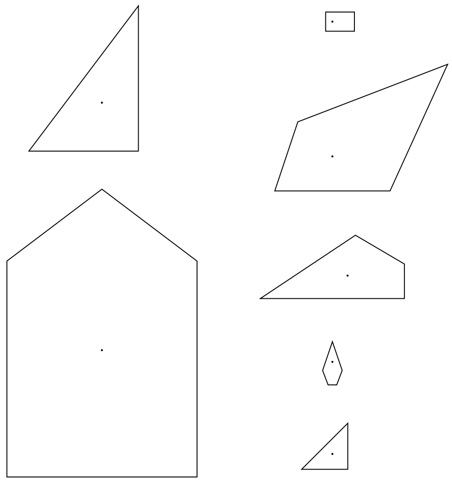

Figure 14: Example parts that planners were tested on.

A part with s sometimes-stable edges has up to 2^s qualitative shapes. Conceptually treat this as an orienting problem where each qualitative shape is a different part. For each qualitative shape, we find its resting ranges, and compute the action ranges for each of its stable and sometimes-stable states. For every state that is stable or sometimes-stable, we overlap its action ranges over all qualitative shapes to compute its composite action ranges. We compute the overlap ranges for a set of indistinguishable states using the composite action ranges for the individual states. From the overlap ranges, we find representative actions and perform breadth-first AND/OR search to find a plan.

9 Implementation

We implemented sensor-based and sensorless planners for orienting with shape uncertainty in Common Lisp. These planners currently generate plans for parts that have a single qualitative shape. Given a nominal part shape, radius values of the center of mass and vertex uncertainty circles, and maximum sensor noise, they return a plan when they can find one and indicate failure otherwise.

The sensor-based planner performs breadth-first AND/OR search to generate sensor-based orienting plans for parts with shape uncertainty. For the parts in Figure 14, going from top to bottom, left to right, the sensor-based planner took an average of 0.192 secs, 1.870 secs, 0.756 secs, 0.262 secs, 0.262 secs, 0.224 secs, and 0.188 secs respectively on a SPARC ELC. The sensorless planner uses breadth-first search to find sensorless orienting plans. See Figure 11 for an example plan. Sensor-based orienting plans can typically handle greater shape uncertainty than sensorless orienting plans.

We tested sensor-based and sensorless orienting plans with shape uncertainty using an Adept 550 robot and conveyor on the set of triangles shown in Figure 15. We ran 30 trials of the sensor-based plan, with 10 trials for each part. We also ran 15 trials of the sensorless plan (Figure 11), with

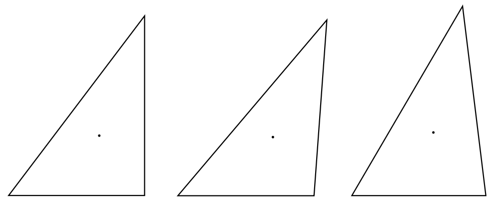

Figure 15: Parts used in experiments. Going left to right, the nominal triangle, triangle with r_v and r_c of 1 mm, and triangle with r_v and r_c of 2 mm. Nominal length of the longest edge is 63.2 mm.

5 trials for each part. Both plans succeeded on all trials.

10 Conclusion

Developing techniques to manipulate parts manufactured to tolerances is important for automated manufacturing. In this paper, we explored the orienting of parts with shape uncertainty and showed that shape uncertainty introduces nondeterminism. We demonstrated that it is possible to generate reliable sensor-based and sensorless orienting plans in the presence of shape uncertainty and characterized a class of parts that can be oriented under shape uncertainty. A similar approach can be applied to other tasks such as orienting by parallel-jaw grasping (Goldberg [11]; Rao and Goldberg [17]) and orienting with actuated fences (Akella *et al.* [2]).

Future work in orienting parts with shape uncertainty includes analyzing a broader class of parts and developing shape uncertainty models that faithfully capture variations in manufactured parts. Generating plans that orient a part or recognize when they cannot orient it would be useful when we cannot find a guaranteed plan. Such plans, similar to Donald's [9] error detection and recovery plans, can potentially handle larger values of shape uncertainty and a broader class of parts, and may even be used as metrological tools to identify parts that do not meet tolerance specifications. Randomized strategies (Erdmann [10]) can be effective in handling the nondeterminism when some states have distinct sensor values. We can also use manufacturing process knowledge to estimate the shape uncertainty parameters and generate plans that minimize the expected execution length.

Acknowledgments

Funding was provided by NSF under grants IRI-9213993 and IRI-9318496 (with ARPA).

References

[1] S. Akella. *Robotic Manipulation for Parts Transfer and Orienting: Mechanics, Planning, and Shape Uncertainty*. PhD thesis, The Robotics Institute, Carnegie Mellon University, Dec. 1996. Robotics Institute Technical Report CMU-RI-TR-96-38.

[2] S. Akella, W. H. Huang, K. M. Lynch, and M. T. Mason. Sensorless parts orienting with a one-joint manipulator. In *IEEE International Conference on Robotics and Automation*, pages 2383–2390, Albuquerque, NM, Apr. 1997.

[3] S. Akella and M. T. Mason. Parts orienting with partial sensor information. In *IEEE International Conference on Robotics and Automation*, Leuven, Belgium, May 1998.

[4] *Dimensioning and Tolerancing, Y14.5M-1994*. American Society of Mechanical Engineers, New York, 1995.

[5] R. C. Brost. Personal communication, 1994.

[6] M. Caine. The design of shape interactions using motion constraints. In *IEEE International Conference on Robotics and Automation*, San Diego, CA, May 1994.

[7] J. Chen, K. Y. Goldberg, M. H. Overmars, D. Halperin, K. F. Bohringer, and Y. Zhuang. Shape tolerance in feeding and fixturing. In *Third Workshop on Algorithmic Foundations of Robotics*, Mar. 1998.

[8] Y.-B. Chen and D. J. Ierardi. The complexity of oblivious plans for orienting and distinguishing polygonal parts. *Algorithmica*, 14:367–397, 1995.

[9] B. R. Donald. Planning multi-step error detection and recovery strategies. *International Journal of Robotics Research*, 9(1):3–60, Feb. 1990.

[10] M. Erdmann. Randomization for robot tasks: Using dynamic programming in the space of knowledge states. *Algorithmica*, 10(2/3/4):248–291, 1993.

[11] K. Y. Goldberg. Orienting polygonal parts without sensors. *Algorithmica*, 10(2/3/4):201–225, 1993.

[12] L. Joskowicz, E. Sacks, and V. Srinivasan. Kinematic tolerance analysis. In J.-P. Laumond and M. Overmars, editors, *Algorithms for Robotic Motion and Manipulation*, pages 401–418. A. K. Peters, Wellesley, Massachusetts, 1997.

[13] L. Kavraki. Part orientation with programmable vector fields: Two stable equilibria for most parts. In *IEEE International Conference on Robotics and Automation*, pages 2446–2451, Albuquerque, NM, Apr. 1997.

[14] J.-C. Latombe, R. H. Wilson, and F. Cazals. Assembly sequencing with toleranced parts. *Computer Aided Design*, 29(2):159–174, 1997.

[15] M. T. Mason. Mechanics and planning of manipulator pushing operations. *International Journal of Robotics Research*, 5(3):53–71, 1986.

[16] F. P. Preparata and M. I. Shamos. *Computational Geometry: An Introduction*. Springer-Verlag, 1985.

[17] A. S. Rao and K. Y. Goldberg. Shape from diameter: Recognizing polygonal parts with a parallel-jaw gripper. *International Journal of Robotics Research*, 13(1):16–37, Feb. 1994.

[18] A. A. G. Requicha. Toward a theory of geometric tolerancing. *International Journal of Robotics Research*, 2(4):45–60, 1983.

[19] R. H. Taylor, M. T. Mason, and K. Y. Goldberg. Sensor-based manipulation planning as a game with nature. In R. C. Bolles and B. Roth, editors, *Robotics Research: The Fourth International Symposium*, pages 421–429, Cambridge, MA, 1988. MIT Press.

[20] H. Voelcker. A current perspective on tolerancing and metrology. *Manufacturing Review*, 6(4):258–268, Dec. 1993.

[21] C. K. Yap. Exact computational geometry and tolerancing metrology. In *Snapshots of Computational and Discrete Geometry, Volume 3*, Sept. 1995. McGill School of Computer Science Tech. Report No. SOCS-94.50.